

Laboratory Investigation of the Dynamics of the Inelastic Bouncing Ball

Jacob Yunis

Aerospace Systems Design Lab, Guggenheim School of Aerospace Engineering,
Georgia Institute of Technology, Atlanta, Georgia 30332, USA

(Dated: 16 December 2011)

An inelastic bouncing ball driven by an oscillating plate is modelled in MatLab and then experimentally investigated in the laboratory. Experimental results qualitatively match the computational model, demonstrating bifurcation and chaos. Discrepancies of the physical system are clearly traced, including friction, elasticity, and feedback, but only friction is accounted for in the model. Further work that accounts for the discrepancies is feasible and recommended.

I. INTRODUCTION

The inelastic bouncing ball presents a simple system for studying chaotic behavior in the laboratory. The ball is driven vertically by an oscillating plate and the observed flight times of the ball are recorded. The periodization of the flight times as a function of the acceleration of the plate exhibits a wide variety of behaviors, including chaos.

The equations of motion of the system were partially resolved by Luck and Mehta for cases with flight times greater than the forcing period¹. Gilet, et. al. fully resolved the equations of motion for both the plate and the ball in². Using A as amplitude, g as the acceleration due to gravity, t as time, ω as frequency, and x as position, the following nondimensionalized variables are phase, generalized position, and reduced acceleration,

respectfully:

$$\varphi = \omega t \quad (1)$$

$$\chi = x\omega^2/g \quad (2)$$

$$\Gamma = \frac{A\omega^2}{g} \quad (3)$$

The position of the plate and ball are described with the following equations (φ_0 represents the first time the ball leaves the plate in each set of flights):

$$\chi_p(t) = \Gamma \sin \varphi \quad (4)$$

$$\chi_b(t) = \Gamma (\sin \varphi_0 - \sin \varphi) + \Gamma \cos \varphi_0 (\varphi - \varphi_0) + \frac{(\varphi - \varphi_0)^2}{2} \quad (5)$$

The takeoff condition for the ball, that is, when the ball leaves the plate, occurs when the reduced acceleration is equal to or greater than 1:

$$\chi_b(t) = \Gamma \sin \varphi \geq 1 \quad (6)$$

This says that the ball takes off when the plate's acceleration exceeds the acceleration due to gravity. This also defines the sticking region and the bouncing region. The sticking region is below the takeoff line ($\Gamma \sin \varphi = 1$), while the bouncing region is above the takeoff line. When the ball lands in the sticking region, it will ride the plate until it crosses the takeoff line, at which point it will leave the plate. If the ball lands in the bouncing region, it will immediately leave the plate.

The time of flight is defined as the time between leaving and contacting the plate:

$$T = \varphi_i - \varphi_0 \quad (7)$$

The time of flight is calculated by solving the following force balance equation for $F = 0$:

$$F = \frac{1}{2}T^2 + \Gamma \cos \varphi_0 (T + \cos T) - \Gamma \sin \varphi_0 (1 - \sin t) = 0 \quad (8)$$

A period- n motion involves n different flights. If the ball lands in the sticking region and rides the plate up to the takeoff line, the periods are reset, and the takeoff of the ball is essentially the same as the first flight. Bifurcation occurs when the motion of the plate causes the ball to impact the plate at a slightly different location. This can cause the ball to cross the takeoff line and enter or leave the sticking region, and greatly alter the dynamics of the ball. For a thorough analysis of

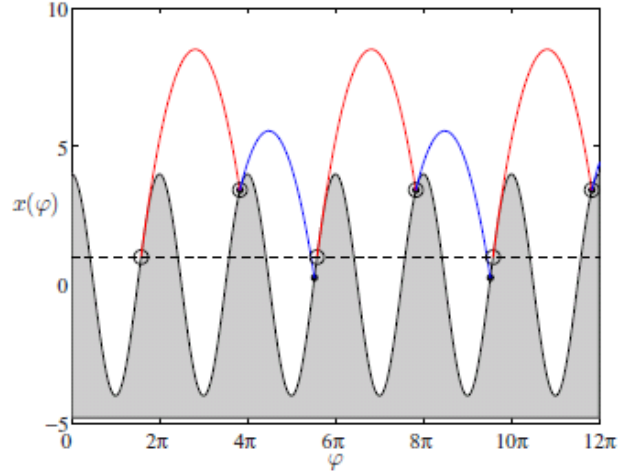


FIG. 1: Fig. 1 from Gilet, et al. showing the takeoff line.

the theoretical motion of the ball, see Gilet, et al.².

The theoretical model described above was coded into MatLab and produced the bifurcation diagram seen in Fig 2, consistent with Figure 2 of Gilet, et al.

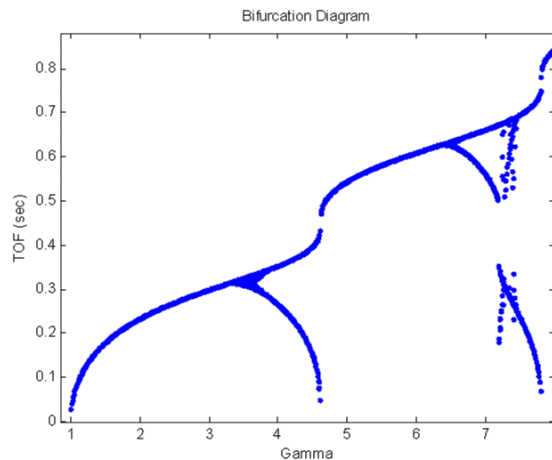


FIG. 2: Bifurcation diagram produced using computational model.

II. METHODS

In order to set up an inelastic bouncing ball system in the lab, we had to overcome 3 primary challenges: using a truly inelastic ball, constraining the ball to 1D motion, and accurately calculating the time of flight.

Initially, a sand filled bag on a driven plate surrounded by a plastic fence was used, see Fig 3a. An accelerometer in the driven plate was used to calculate flight time. The input sine wave determined the takeoff point by calculating the takeoff line. The input sine wave was then subtracted out of the accelerometer signal to calculate the landing point. This signal was too noisy to be of use (Fig 4) and the ball did not consistently remain in the center of the plate.

The lab setup was then reconfigured (Figure 3b). A metal block ($m = 249$ g) with ball bearings was attached to a vertical pole to stabilize the motion in 1-D. This came at a cost of friction of the mass on the pole and slight elasticity of the mass. The friction was assumed to be Coulomb friction: constant with and opposite in sign to velocity. The friction was observed to be approximately $0.29g$. The takeoff times were calculated using an electrical circuit which was grounded at $x = 0$. The resulting signal provided very precise takeoff times (Figure 5). The coefficient of restitution of the mass was

observed to be $c_R \approx 0.515$. The friction was incorporated into the computational model developed in the Introduction, however the c_R was not, due to time constraints. Other experimental issues include the slight twisted of the mass due to nonuniform impact with the plate and low frequency shaker oscillation cause by feedback from the mass striking the plate at high Γ .

Data was collected at a sample rate of 20 KHz. The frequency of the plate was held constant during a run; the amplitude of the plate was altered to produce varying Γ . The frequency was varied between 20 and 40 Hz from run to run. The amplitude was stepped up gradually from $\Gamma = 0$ to $\Gamma = 8$ using a constant stepwise function. Different strategies were used to try to limit transients in the dynamics due to changing Γ . The optimal setup was to examine small ranges of Γ at a time, with between 50 and 100 oscillations at each Γ . In addition, the first 10 oscillations at each Γ thrown out to allow the system to settle.

III. RESULTS

The data collected produced very reasonable results. Figure 7 displays the collected data next to our predicted model. The data is less noisy for lower Γ because there was less feedback from the shaker oscillating due

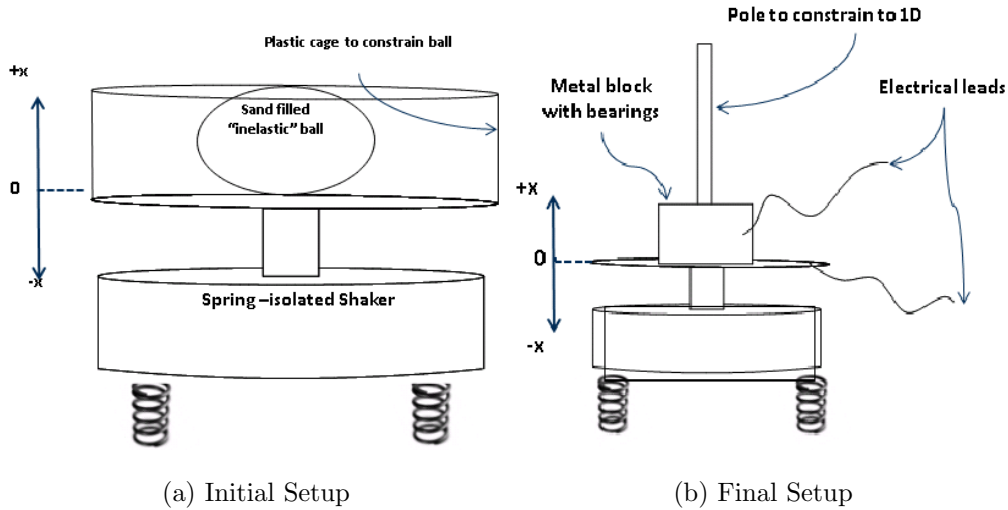


FIG. 3: Lab Setups

to mass strikes. A return map was created for several Γ (Fig. 8). The time of flights can be seen moving from single period to period doubling to chaos as Γ rises. An interesting bimodal shape appears at high Γ . Errors in time of flight tended to be on the order of

$\frac{1}{2}$ to $\frac{2}{3}$ times the predicted flight times.

IV. DISCUSSION

Examining Figure 7, the experimental data collected closely matches the expected behavior of the system. The results en-

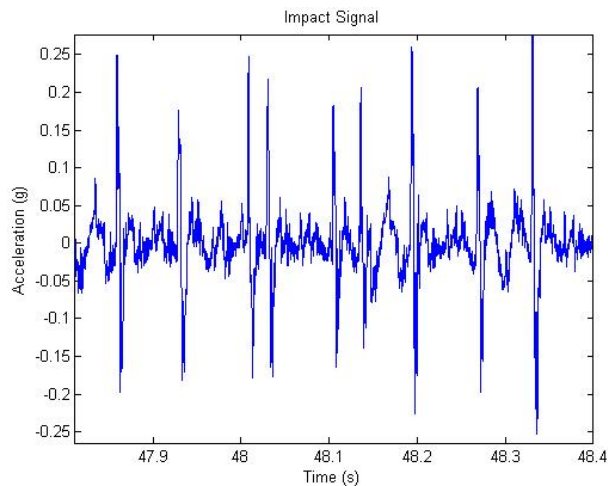


FIG. 4: Noisy accelerometer signal used to calculate flight time discarded for inaccuracy.

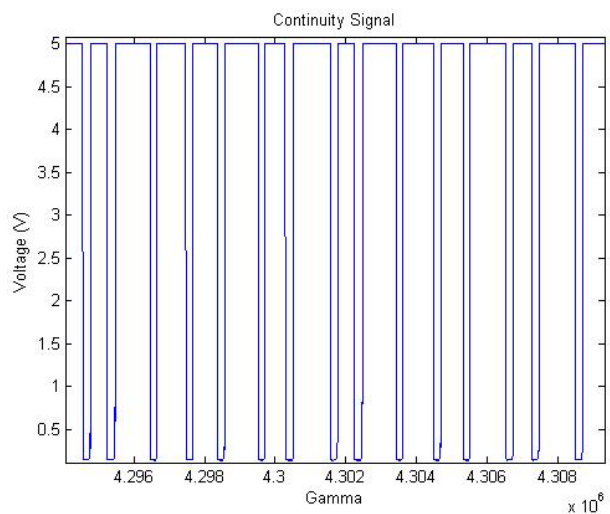


FIG. 5: Noiseless continuity signal used to calculate flight time in final setup.

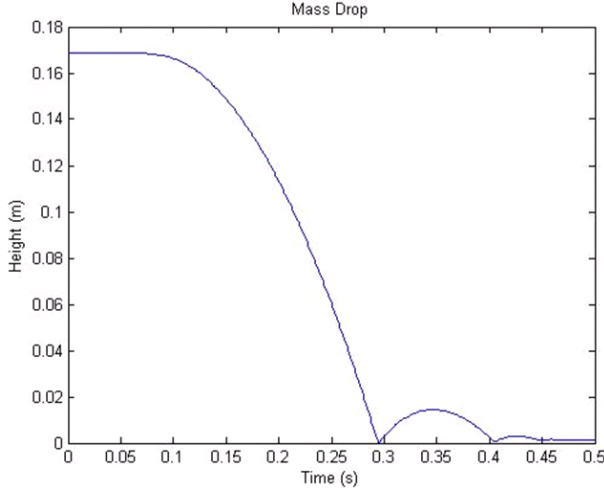


FIG. 6: Drop test used to calculate friction and c_R .

courage the further development of the experimental setup to demonstrate chaos in a laboratory setting. The shape of the maximum time of flight follows the computational model. The forbidden areas are clearly seen in the full range bifurcation diagram (Fig. 7c). The initial bifurcation occurs at slightly less than $\frac{1}{2}\Gamma$ before predicted, and with T of slightly less than $\frac{1}{2}$ the predicted T . See below for a discussion of the data gap between $\Gamma = 1.75$ to $\Gamma = 1.95$ and $\Gamma = 4.55$ to $\Gamma = 4.85$.

The three primary experimental distinctions from the ideal system are the friction of the mass on the post, the elasticity of the mass bouncing on the plate, and the low frequency oscillation of the shaker at high Γ .

Figure 9 shows the change in bifurcation diagram when the Coulomb friction was in-

corporated into the computational model. This brings the experimental bifurcation diagram closer to the computational diagram.

The friction of the post removes energy from the mass, but the elasticity of the mass adds energy to the mass (compared to the computational model). The energy added, however, is insignificant compared to the energy lost due to friction. The c_R may vary with velocity, however further tests were not conducted.

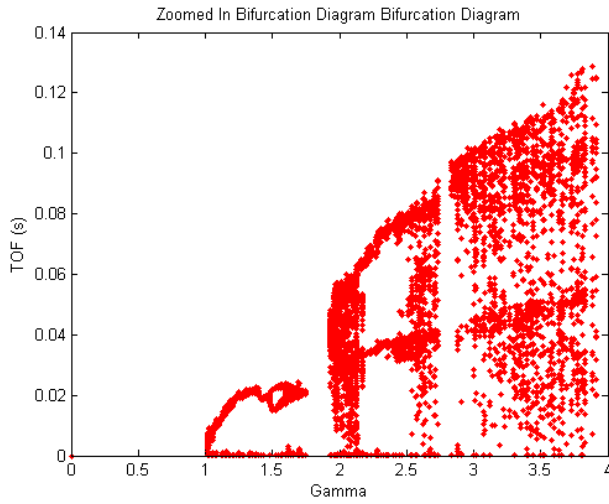
Energy lost due to friction at $\Gamma = 3.4, T = 0.11s$:

$$0.0122 \text{ J}$$

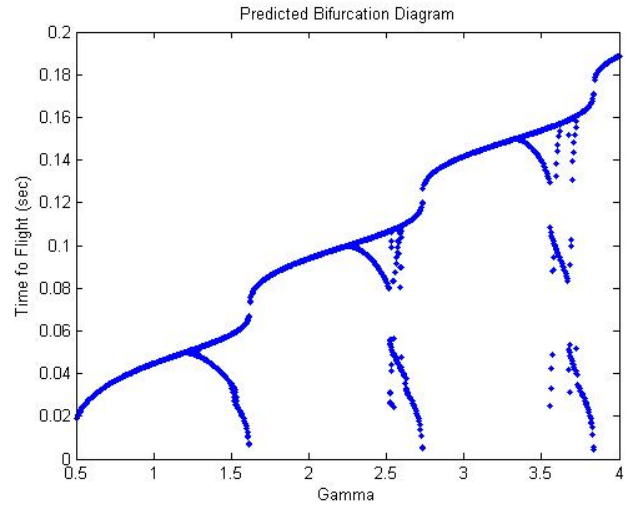
Energy gained due to $c_R = 0.515, T = 0.11s$ (from friction drop test):

$$0.00498 \text{ J}$$

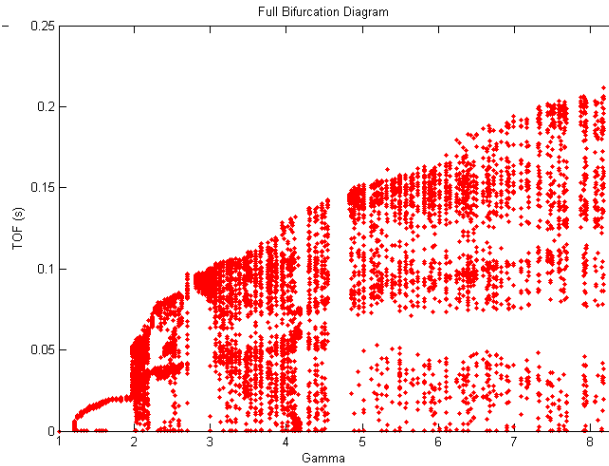
The shaker exhibited clear visual signs of oscillation near $\Gamma = 6$, however, the affects of the shaker oscillation probably began influencing the data before the oscillation was visible. An interesting correlation is noted in Figure 10. It contains the bifurcation diagram using a computational model that incorporates integer multiples of the driving frequency superpositioned on the original input signal. This shows remarkable similarity to the experimental results beyond $\Gamma \approx 2$. The strange vertically oriented forbidden zones in the experimental data, which do not



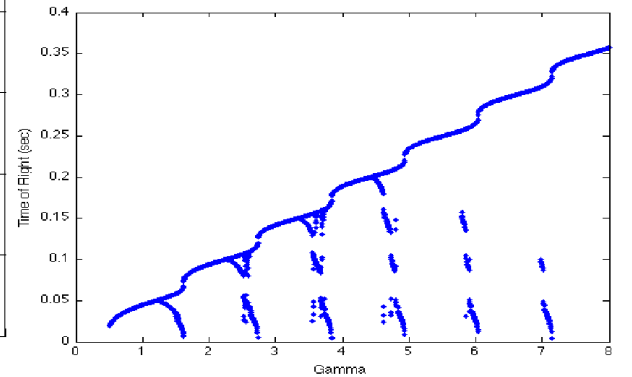
(a) Data $\Gamma = 0 : 4$



(b) Model $\Gamma = 0 : 4$



(c) Data $\Gamma = 0 : 8$



(d) Model $\Gamma = 0 : 8$

FIG. 7: Collected data in bifurcation diagrams compared to models.

appear in the original model, suddenly appear in the model which incorporates the additional harmonic sine wave. Although the input signal of the plate is not an exact harmonic of the shaker oscillation, it is closely related because the motion of the shaker is driven by the impact of the falling mass. This produces an effect similar to the bifurcation

diagram modeling a sine wave with the third harmonic superimposed.

V. CONCLUSION

The inelastic bouncing ball system is a simple 1D system to model. Creating the system in a lab is slightly more difficult, how-

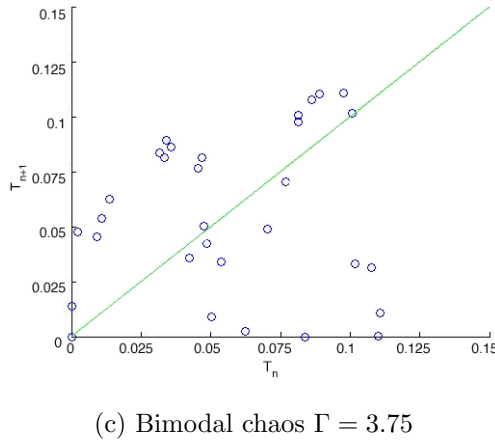
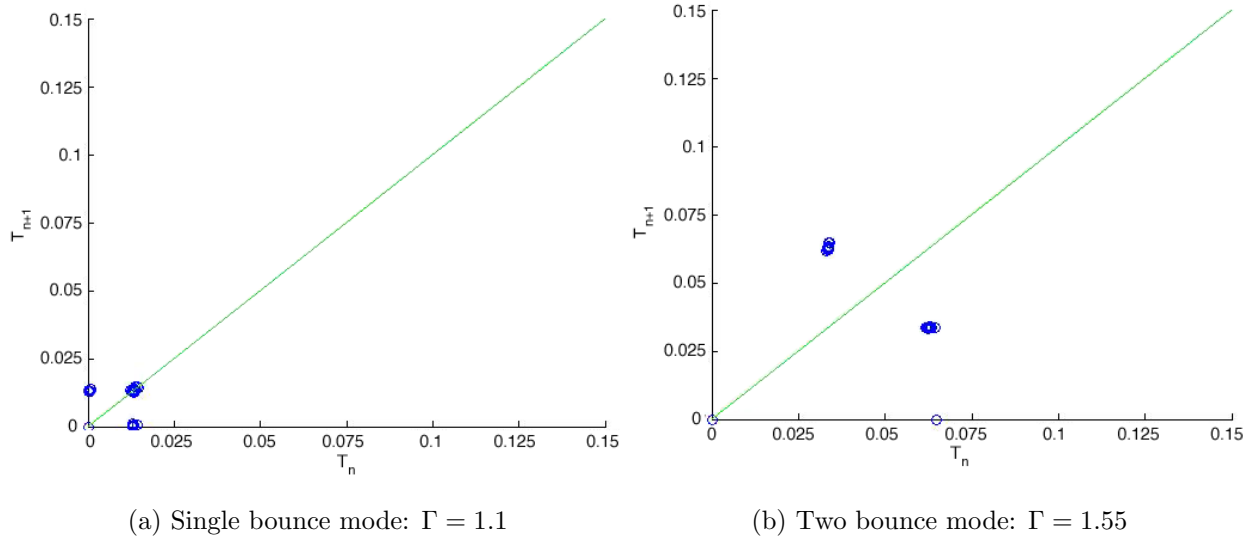


FIG. 8: Return maps at 3 different Γ values (From data set $\Gamma = 0 : 4$).

ever, this paper proves the feasibility of execution. The experimental data obtained in the lab correlated well, if not precisely, with the computational model. Bifurcations in time of flight were clearly present. At higher Γ , feedback from the mass hitting the platform created an effect similar to superimposed harmonic sine waves. Also, chaos was present at higher Γ , as demonstrated by the return maps. Further work would include

tuning the lab setup to eliminate the elasticity of the mass and reduce the friction on the pole. More precise calculation of friction and the c_R would also enable better matching of the model to the data. Lastly, measuring the feedback oscillation of the shaker would allow a precise bifurcation diagram to be produced. These modifications would require only moderate effort.

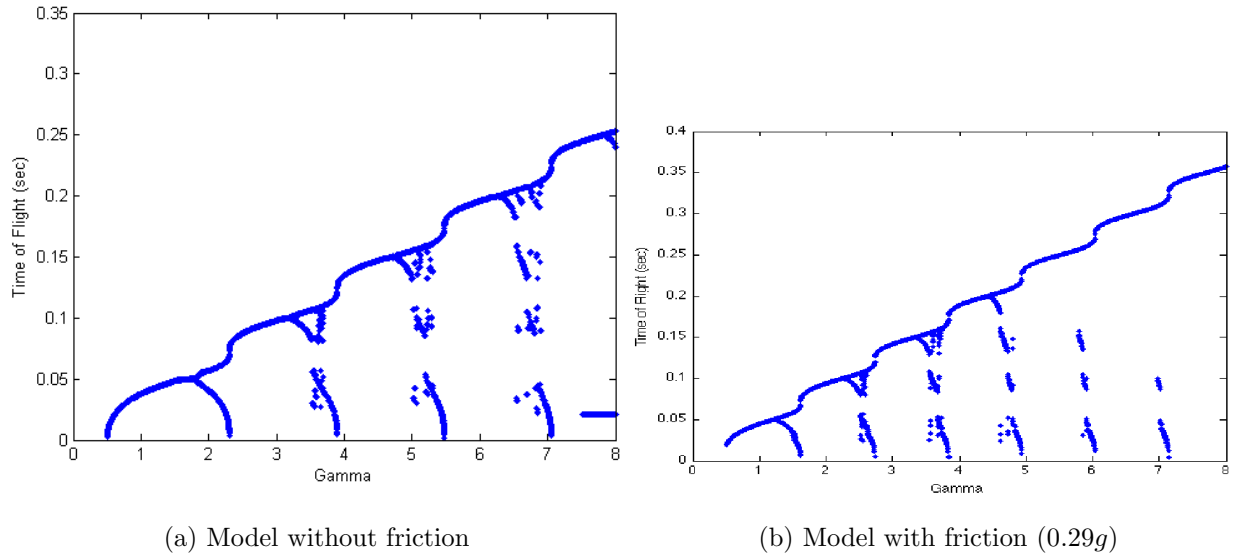


FIG. 9: Change in model from including Coulomb friction.

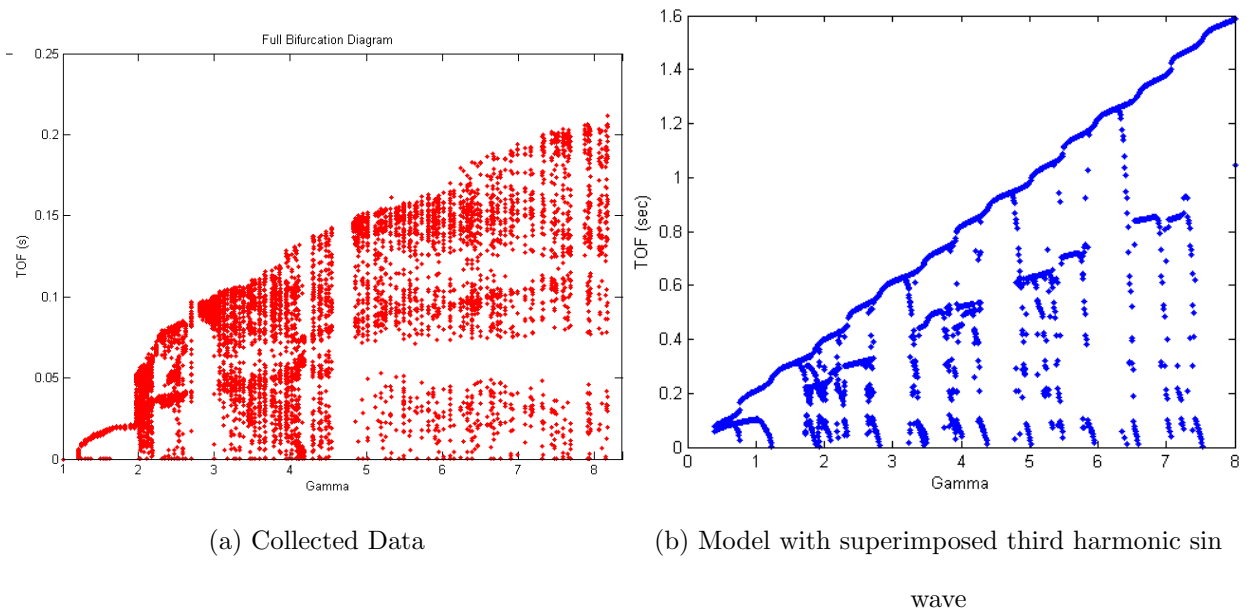


FIG. 10: Effect of low frequency shaker oscillation compared to harmonics of input sine wave.

Lastly, when the project was originally planned, the experiment included the laboratory examination of different superimposed harmonic sine waves. The lab equipment was not capable of this analysis at the time of experimentation, however the computer model proved useful in analyzing the data and discrepancies. A worthwhile extension of this project might also include the effect of multiple sine waves.

REFERENCES

- ¹Anita Mehta and J. M. Luck. Novel temporal behavior of a nonlinear dynamical system: The completely inelastic bouncing ball. *Phys. Rev. Lett.*, 65:393–396, Jul 1990.
- ²T. Gilet, N. Vandewalle, and S. Dorbolo. Completely inelastic ball. *Phys. Rev. E*, 79:055201, May 2009.